LASER & PHOTONICS REVIEWS

www.lpr-journal.org

Optical Anomalies due to Volume Collective Modes of Plasmonic Metamaterials

Danielle Ben-Haim and Tal Ellenbogen*

The emergence of optical anomalies in 3D plasmonic metamaterials upon excitation of volume collective modes is studied. These modes engage a collective response of all the meta-atoms across the volume of the structure and arise due to coupling of localized plasmonic modes with Bloch modes of the 3D lattice. Two types of volume collective modes are introduced; a reflective mode resilient to the plasmonic absorption, exhibiting reflection that approaches unity with extremely low loss, through a distinct high-Q spectral locking of the response of all the constituent plasmonic resonators in the volume; in addition, a transmissive mode that supports the emergence of lattice matched scattered waves within the volume, leading to full transmission through a spectral transparency window. These attractive optical properties of the volume collective modes may lead to a breakthrough in the design of low-loss and efficient 3D plasmonic metamaterials for novel linear and nonlinear photonic applications.

1. Introduction

Optical metamaterials have been extensively studied over the past two decades due to their potential to control and manipulate light in ways that cannot be matched by naturally grown materials.[1,2] These nano-engineered materials are built from subwavelength inclusions called meta-atoms. The individual properties of the meta-atoms govern the metamaterial optical response, which can be tuned by a specific design of the meta-atom's shape, material, and orientation. Furthermore, the optical response strongly depends on the distribution of the meta-atoms in space, and particularly on how they interact with one another when excited by light. The periodic arrangement of the meta-atoms in 1D, 2D, or 3D lattices can lead to coherent excitation through Bloch modes and give rise to collective phenomena that exhibit strong resonances and enhanced light-matter interaction.[3–13]

The use of metallic nanoparticles as meta-atoms has proved to be highly advantageous, due to a wide range of associated optical phenomena such as magnetic resonances, optical chirality, hyperbolic dielectric response, geometric phase, and optical nonlinearities.[2,14–18] These phenomena have contributed to the realization of plasmonic metamaterials with diverse capabilities, mainly in planar metasurfaces that have also extended to multilayered platforms.[19–23] Nevertheless, despite all the benefits of plasmonic metamaterials, a major drawback comes from the inherent losses to absorption in the metal.[24] Particularly subwavelength metallic nanoparticles, excited with a localized mode known as localized surface plasmon (LSP), exhibit strong absorption that peaks at the resonance. These losses pose limitations on the performance of plasmonic metamaterials and thus require advanced approaches to mitigate the loss.

Here we demonstrate how 3D plasmonic metamaterials can be properly designed to give rise to volume collective modes that exhibit anomalous optical behavior with extremely low losses. These loss-protected modes are associated with coherent interactions between the plasmonic meta-atoms, which extend throughout the entire volume of the structure. Therefore, they are fundamentally different from localized modes (at a single particle) or surface lattice modes (at a single surface).[25,26] As we show below, the volume collective modes arise when the Bloch modes of a 3D lattice couple to the LSP mode of the constituent meta-atoms under quasi-momentum conservation. We examine two distinct types of modes that exhibit different optical phenomena. The first type is a reflective mode, analogous to Bragg mode, in which the light is coherently scattered backward. We show that in spite of the absorptive nature of the plasmonic resonators, this volume collective mode exhibits a significant reduction in absorption, that counter-intuitively continues to decrease as the metamaterial size increases. In addition, it manifests in perfect locking of the plasmonic resonators response over the entire volume of the metamaterial, regardless of its size or depth. The second type is a transmissive mode, in which coherent interactions along the direction of a certain reciprocal lattice vector lead to a

D. Ben-Haim, T. Ellenbogen
Department of Physical Electronics, School of Electrical Engineering
Tel-Aviv University
Tel-Aviv 6779801, Israel
E-mail: danielleb2@mail.tau.ac.il

D. Ben-Haim, T. Ellenbogen
Center for Light-Matter Interaction
Tel-Aviv University
Tel-Aviv 6779801, Israel

The ORCID identification number(s) for the author(s) of this article can be found under https://doi.org/10.1002/lpor.202200671

DOI: 10.1002/lpor.202200671

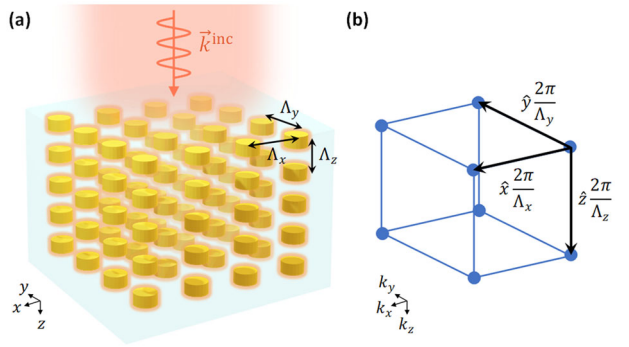

Figure 1. a) Excitation of volume collective modes in a 3D nano-engineered metamaterial. The metamaterial is illuminated by incoming light that leads to coherent excitation of the nanoparticles through quasi-momentum conservation in a 3D lattice with periodicities Λ_x, Λ_y and Λ_z. b) The three corresponding reciprocal lattice vectors in k-space.

spectral transparency window that can be considered as the volume counterpart to the surface lattice resonance phenomenon that occurs in 2D metasurfaces.

2. Semi-Analytical Model

We study a metamaterial structure consisting of identical plasmonic nanoparticles embedded in a dielectric medium. Without loss of generality, the particles are arranged in a simple 3D lattice, where the lattice vectors are aligned to the cartesian coordinate system, as illustrated in **Figure 1**. We consider a metamaterial that is finite in the z-direction and is assumed to be laterally large enough relative to the wavelength to be considered infinite in the x and y directions. Therefore, it can be analytically treated as a finite stack of metasurface layers. We study the system under the coupled-dipole approximation (CDA),[27] where we consider a dipolar response of each meta-atom and neglect higher multipoles. The metamaterial is illuminated by a plane wave that excites the nanoparticles and induces in each nanoparticle a dipole moment that depends on its polarizability tensor $\boldsymbol{\alpha}_s$ and its local field $\vec{E}^{loc}$, according to:

$$\vec{p}_{nml} = \boldsymbol{\alpha}_s \vec{E}^{loc}\left(\vec{r}_{nml}\right),\ n,m,l = 0,\pm1,\cdots \tag{1}$$

where $\vec{p}_{nml}$ is the dipole moment of a particle located in $\vec{r}_{nml} = n\Lambda_x\hat{x} + m\Lambda_y\hat{y} + l\Lambda_z\hat{z}$. Under plane-wave excitation of a stack of infinite periodic arrays, with the same periodicity in x and y directions, all dipoles in each layer will have the same dipole moment strength with different phases that correspond to the transverse phase of the incident field:

$$\vec{p}_{nml} = \vec{p}_l\ \exp\left(i\vec{k}_{\parallel}^{inc}\cdot\vec{r}_{nm}\right) \tag{2}$$

where $\vec{k}_{\parallel}^{inc}$ is the transverse wavevector of the incident field, $\vec{r}_{nm} = n\Lambda_x\hat{x} + m\Lambda_y\hat{y}$ is the particle's transverse location, and $\vec{p}_l$ is the induced dipole moment of the l-th metasurface layer.

The local field at the nanoparticle's location accounts for both the incident field and the scattered fields from all other dipoles in the structure. Therefore, the dipole moment of the l-th layer is described by the following equation:

$$\vec{p}_l = \boldsymbol{\alpha}_s\left[\vec{E}_0^{inc}\exp\left(ik_z^{inc}z_l\right) + \mathbf{G}_l\vec{p}_l + \sum_{i\neq l}\mathbf{G}_{i\to l}\vec{p}_i\right] \tag{3}$$

where $\vec{E}_0^{inc}$ is the incident field amplitude, k_z^{inc} is the $\hat{z}$ component of the incident wavevector, z_l is the location of the l-th layer on the z–axis, $\mathbf{G}_l$ is the sum of scattered field contributions to a particle located in layer l from all other particles at that layer, and $\mathrm{G}_{i\to l}$ is the sum of scattered field contributions to a particle located in layer l from all the particles in layer i. The scattered field contributions from the dipoles are calculated using Green's function. Equation (3) can be rearranged as the following linear set of equations:

$$\sum_{i=1}^{N}\begin{Bmatrix}\boldsymbol{\alpha}_s^{-1} - \mathbf{G}_l, & i = l\\ -\mathbf{G}_{i\to l}, & i\neq l\end{Bmatrix}\vec{p}_i = \vec{E}_0^{inc}\ \exp\left(ik_z^{inc}z_l\right),\ l = 1,\ldots,N \tag{4}$$

whose solution provides the dipole moments of each metasurface layer in the stack. The total scattered field observed at a certain point is the sum of contributions from all particles in the structure. Since the structure is assumed infinite in the x and y directions, the far field contains backward and forward scattered plane waves from each layer, and the reflection and transmission from the entire structure are calculated from the zeroth-order diffraction.[28] The CDA method allows us to numerically calculate the dipole moments of the stacked metasurfaces, given the incident wave and the single-particle polarizability tensor. For the case of nanodisks as the constituent meta-atoms, the polarizability tensor is diagonal and symmetric, such that $\alpha_{xx} = \alpha_{yy} \gg \alpha_{zz}$. The diagonal terms of the polarizability can be approximated by a Lorentzian lineshape that describes the resonant LSP modes that can be excited in the nanodisk.[29]

Although the studied metamaterial is finite and externally excited, the Bloch modes of the corresponding 3D lattice provide further insight into its physical behavior. The Bloch modes sustained by the 3D lattice are given in terms of the following quasi-momentum conservation condition with the three reciprocal lattice vectors in k-space:

$$\left|\vec{k}_{uvw}^{sc}\right| = k,\ \vec{k}_{uvw}^{sc} = \vec{k}^{B} + u\frac{2\pi}{\Lambda_x}\hat{x} + v\frac{2\pi}{\Lambda_y}\hat{y} + w\frac{2\pi}{\Lambda_z}\hat{z} \tag{5}$$

where k is the background wavenumber, $\vec{k}^{B}$ is the Bloch wavevector, uvw are integers and stand for the order of diffraction, and $\vec{k}_{uvw}^{sc}$ is the corresponding scattered wavevector. In an infinite periodic 3D lattice, all nanoparticles have the same dipole moment strength, differ only by a phase factor that corresponds to the Bloch wave phase at the nanoparticles' location:

$$\vec{p}_{nml} = \vec{p}\ \exp\left(i\vec{k}^{B}\cdot\vec{r}_{nml}\right) \tag{6}$$

In the finite metamaterial, the same collective behavior is supported by the eigenmodes of the system, that arise at the momentum matching condition of the Bloch modes in Equation (5),

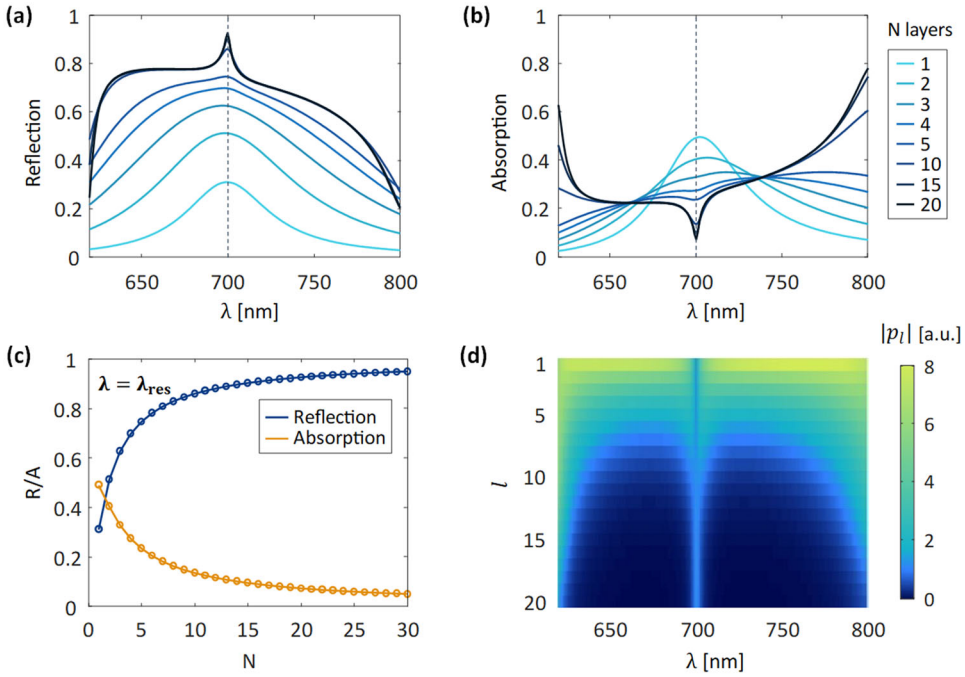

Figure 2. a) Reflection and b) absorption spectra from a metamaterial with increasing number of layers N, designed to exhibit a reflective type of volume collective mode at the resonance wavelength $\lambda_{res} = 700$ nm, with periodicities $\Lambda_x = \Lambda_y = 300$ nm and $\Lambda_z = \lambda_{res}/2\, n_b = 240$ nm. c) Reflection and absorption at the resonance wavelength as function of N. d) Dipole moment amplitude for a structure of 20 layers, as function of the wavelength and the layer's index *l*. Taken from CDA calculations.

where $\vec{k}^{B}$ is replaced by the incident wavevector $\vec{k}^{inc}$. These are the volume collective modes of the metamaterial, which exhibit coherent excitation of all nanoparticles across the volume. Different types of volume collective modes can be excited, depending on the excitation conditions that give rise to a different optical behavior. In the following section, we will examine two distinct types of such modes and characterize their unique optical properties.

3. Results and Discussion

The first studied type of volume collective mode arises when the reciprocal lattice vector along the *z*-direction allows for momentum matching with a backward scattered wave, according to Equation (5), which corresponds to Bragg's condition. For normal incidence $\vec{k}^{inc} = k\hat{z}$, the collective mode is excited with a backward scattered wavevector $\vec{k}^{sc}_{uvw} = -k\hat{z}$ when the lattice periodicity in the *z*-direction equals multiples of half the wavelength:

$$\Lambda_z = q\frac{\lambda}{2n_b},\ q = -w = 1, 2, \ldots \tag{7}$$

where λ is the vacuum wavelength, λ/n_b is the wavelength in the background material, n_b is the background refractive index, and q is the order of the mode. According to Equation (6), the dipole moments of the metasurface layers take the form $\vec{p}_l = \vec{p}\ \exp(i\pi q l)$, such that they are equal in strength with a phase difference of either π (for odd values of q) or 2π (for even values of q).

To study deeper the reflective volume collective mode, we design a metamaterial that supports its excitation for normal incidence, at the collective plasmonic resonance of each single metasurface layer ($\lambda_{res} = 700$ nm). It consists of gold nanodisks with 44 nm radius and 20 nm height, embedded in a silica background. We perform both numerical calculations based on the CDA approach and finite-element simulations of the electromagnetic interaction (in COMSOL Multiphysics). The CDA method can accurately predict both near and far field interactions between the dipole moments excited in the nanoparticles within the metamaterial volume. It can be calculated fast and used to understand the physical dynamics of small and large systems of interacting dipoles. The finite-element simulation goes beyond the dipole approximation. It includes the specific physical characteristics of the nanoparticles and the background material, thus it takes into account retardation effects within the nanoparticles and the interband transitions of gold in the visible regime. In addition, it provides the solution for the fields within the metamaterial structure. The periodicities in each metasurface layer are subwavelength, $\Lambda_x = \Lambda_y = 300$ nm, such that for normal incidence only the zero diffraction order emerges. The periodicity in the *z*-direction is chosen to be $\Lambda_z = \lambda_{res}/2\, n_b = 240$ nm, such that the reflective collective mode of the first order ($q = 1$ in Equation (7)) is excited at the resonance wavelength. **Figure 2**a,b shows the reflection and absorption from the metamaterial structure, for an increasing number of layers, as calculated by the CDA approach. Due to the arrangement of the layers in the Bragg condition at the resonance wavelength, it is expected for the reflection to increase with the number of layers, as seen in Figure 2a. However, there is a counter-intuitive behavior of a significant decrease in the plas-

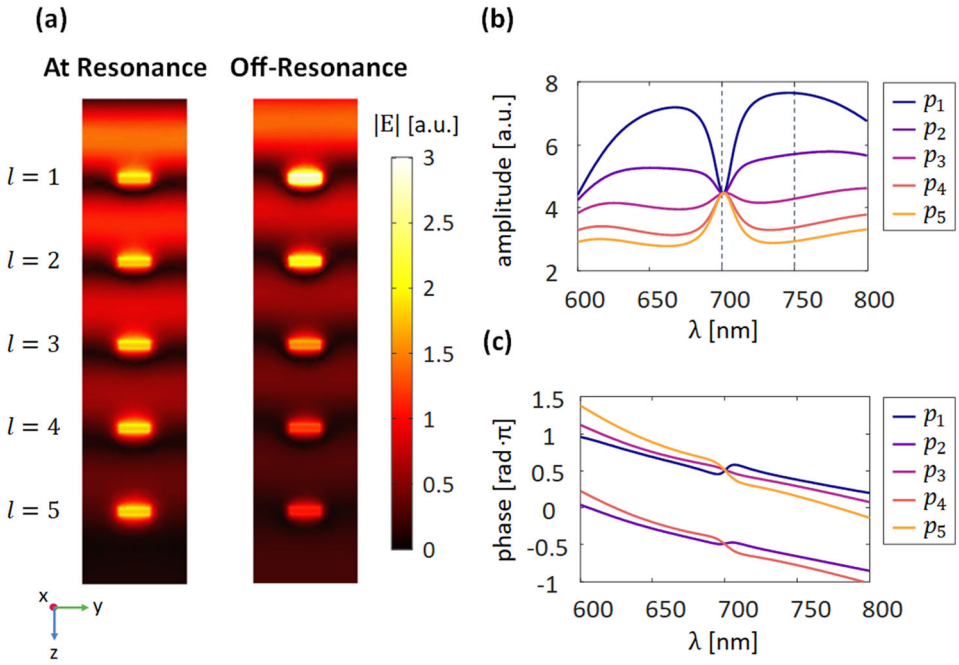

Figure 3. Reflective volume collective mode excited in a metamaterial consisting of 5 layers with periodicities $\Lambda_x = \Lambda_y = 300$ nm and $\Lambda_z = \lambda_{res}/2\, n_b = 240$ nm. a) A cross-section view of the electric field amplitude at the resonance wavelength $\lambda = \lambda_{res} = 700$ nm, and at an off-resonance wavelength $\lambda = 750$ nm, taken from finite-element simulations. b) The amplitude and c) phase of each layer's induced dipole moment, taken from CDA calculations.

monic absorption at the collective mode, as seen in Figure 2b, which accompanies a sharp peak in the reflection as the metamaterial size increases. One might think that by adding more lossy plasmonic layers, the total absorption should increase. Nevertheless, this volume collective mode is anomalously resilient to the assumed absorption. If we look for example at the 20 layers structure, the reflection increases from 0.3 to more than 0.9 while the absorption goes down from 0.5 to below 0.08. The sharp peak in reflection and dip in absorption continue to increase and go down monotonically with the number of layers, as shown in Figure 2c. A similar behavior was previously observed in 3D plasmonic Bragg structures from gold nanowires by Taubert et al.,[20] when studying the limitation of radiative coupling in 3D plasmonic metamaterials. However, the role and peculiarity of the collective mode were not fully discussed. The specific signature of the collective mode is expressed by the ultrasharp spectral features seen in Figure 2a,b that emerge at the resonant wavelength for large enough stacks (>5 layers in the calculated example). It arises due to coupling between the 3D lattice Bloch mode and the LSP mode of the constituent nanoparticles. The strong scattering that originates from the LSP mode is collectively intensified through coherent interactions at the Bloch mode and is thus capable of suppressing the plasmonic absorption. Therefore, as the size of the metamaterial increases, the absorption goes toward zero, and the reflection toward unity, as depicted in Figure 2c. The CDA results in Figure 2a,b were verified by finite-element simulations, depicted in Figure S1, Supporting Information.

The collective behavior of the plasmonic resonators at the volume collective mode is expected to match the Bloch mode of the equivalent 3D lattice, where all the nanoparticles have the same dipole moment strength, according to Equation (6). This behavior can be clearly seen from the dipole moment amplitude, depicted in Figure 2d for a structure of 20 layers. Within the wide spectral band of high reflectivity, where there is an overall decrease of the dipole moment strength with the layer's depth, an extremely narrow band is revealed around the resonance wavelength of the volume collective mode, where the dipole moment is locked and maintains the exact same value across the entire structure. It exhibits an ultrahigh quality factor of the volume collective mode, which is 20 times higher for the 20 layer structure compared to that of the single layer localized mode. This unique phenomenon of spectral locking is manifested by an equal distribution of the excitation power along all the nanoparticles within the metamaterial, regardless of the number of layers.

This intriguing behavior is also observed by finite-element simulations as shown in **Figure 3**a, for a structure of 5 layers. The electric field within the nanoparticles indicates the relative excitation strength of their dipole moments. At the resonance wavelength all layers are excited at the same strength, whereas at an off-resonance wavelength, the strength decreases in the deeper layers. The corresponding amplitude of the layers' dipole moments, calculated by the CDA approach, is shown in Figure 3b. It shows how in the exact spectral point of this volume collective mode, the dipole moments of the different layers align to the same value. In addition, Figure 3c shows the π phase difference in the dipole moments of adjacent layers at the resonance wavelength, as expected for this mode.

Additional insight into the behavior of the reflective collective mode can be gained through an equivalent transmission-line model of the problem,[30] as depicted in **Figure 4**. In this model, each metasurface layer is represented by an effective admittance Y_S, that is derived from the single metasurface properties. The

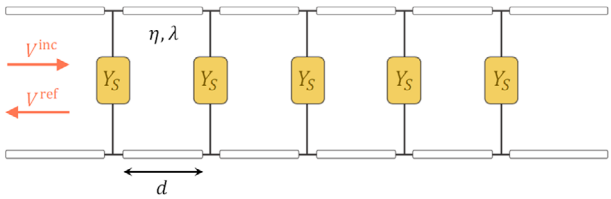

Figure 4. The equivalent transmission-line model for a metamaterial that is based on a stack of 5 metasurfaces, illuminated by normal incident light. Each metasurface layer is described by an effective surface admittance Y_S. The layers are separated by transmission-line segments of length d with characteristic impedance η, and the lines on both ends are infinite. V^{inc} and V^{ref} are the incident and reflected wave amplitudes, respectively.

admittances are connected in parallel to segments of transmission lines of length d, that corresponds to Λ_z. At the resonance wavelength, d equals half the wavelength, and thus the admittance seen at the input of each transmission-line segment equals its load. Overall, the admittance Y_{in} seen by the incident wave is:

$$Y_{in} = N \cdot Y_S + \frac{1}{\eta} \tag{8}$$

where N indicates the number of metasurface layers and η is the impedance of the background material. Hence, the reflection coefficient for N layers is:

$$r_N = \frac{-N \cdot Y_S}{\frac{2}{\eta} + N \cdot Y_S} \tag{9}$$

As N increases, it can be seen from Equation (8) that Y_{in} increases, which reduces the power dissipation on the distributed system, and the reflection $|r_N|^2$ approaches unity. Thus, the equivalent transmission-line model supports the results from the CDA method. As $N \to \infty$ we see that $Y_{in} \to \infty$ (short circuit) and $r_N \to -1$, similar to the reflection from a perfect lossless conductor. It shows that at the resonance wavelength of the volume collective mode, an effectively lossless metamaterial is formed. Furthermore, the voltage V_S that falls on each admittance Y_S is equal in amplitude with a π phase difference, and so is the current that flows through each admittance, since $I_S = Y_S V_S$. This current is proportional to the dipole moment of each metasurface layer,[30] and therefore it coincides with the expected behavior of the reflective collective mode.

Another type of volume collective mode can arise when the momentum matching condition in Equation (5) leads to scattered waves in the direction of a reciprocal lattice vector, due to diffraction of the incoming light. In a single metasurface layer, the emergence of a diffracted wave traveling on the surface is associated with the known phenomenon of Rayleigh anomaly,[31,32] and leads to the excitation of surface lattice resonances, that might cancel the local field at the nanoparticles' location and induce a spectral transparency window.[33] Such lateral diffraction occurs due to momentum matching along the metasurface plane, leading to coherent scattering between the particles on the surface. On the contrary, in the 3D case, not only dipoles on each layer contribute to the local field, but also dipoles at all other layers. Therefore, coherent scattering between the nanoparticles in a 3D lattice requires momentum matching in all directions. In the case of normal incidence, excitation of these lattice matched waves requires the scattered wavevector to contain only the x and/or y reciprocal lattice vectors, and therefore, in order to satisfy the condition in Equation (5), the z-direction reciprocal lattice vector must cancel the incident wave momentum. Thus, the volume collective modes arise at the following condition:

$$\sqrt{\left(\frac{u}{\Lambda_x}\right)^2 + \left(\frac{v}{\Lambda_y}\right)^2} = \frac{n_b}{\lambda},\ \Lambda_z = q\frac{\lambda}{n_b},\ q = -w = 1, 2, \ldots \tag{10}$$

given that the incident polarization state supports the excitation of the corresponding scattered wavevector $\vec{k}^{sc}_{uvw} = u2\pi/\Lambda_x\hat{x} + v2\pi/\Lambda_y\hat{y}$. At this condition, the incident and the scattered waves destructively interfere at the nanoparticles' location and thus the dipole moment of the corresponding polarization state is zero. As a consequence, there are no scattered waves that propagate in the z-direction outside of the structure, which leads to a full transmission of the incident wave within a spectral transparency window.

To look into this transmissive volume collective mode, we design a second metamaterial that supports its excitation, consisting of the same gold nanodisks as before. The lattice periodicities are set such that the first order of this mode ($q = 1$ in Equation (10)) is excited for x-polarized normal incidence at wavelength λ_{res} (in this case $\Lambda_x = 300$ nm and $\Lambda_y = \Lambda_z = \lambda_{res}/n_b = 480$ nm). When the transmissive collective mode is excited, two scattered waves traveling in $+\hat{y}$ and $-\hat{y}$ directions emerge, as they destructively interfere with the incident light at the nanoparticles' location and thus cancel the nanoparticles' dipole moment. This is pronounced by an absorptionless transparency window at the resonance wavelength $\lambda_{res} = 700$ nm, as can be seen in **Figure 5**a, where the transmission equals unity, regardless of the number of layers. On the other hand, Figure 5b shows the response from a stack of the same metasurfaces, however at a different periodicity in the z-direction, such that momentum matching is not achieved in the 3D lattice. Although it can be seen in Figure 5b that the single metasurface layer supports the emergence of a transparency window at λ_{res} (due to a surface lattice resonance), a stack of two or more of these metasurface layers will not excite a transmissive volume collective mode and thus the transparency goes down. Figure 5c shows the transmission at the resonance wavelength as a function of $n_b\Lambda_z/\lambda_{res}$, where transparency windows are observed at the transmissive collective modes that satisfy Equation (10). Furthermore, it can be seen that the collective phenomenon is much more pronounced in the near-field region, and as Λ_z increases, the interactions in the z-direction become weaker and the response is mostly dominated by the surface's collective response. The CDA results in Figure 5a were verified by finite-element simulations, depicted in Figure S2, Supporting Information.

Furthermore, due to the asymmetry in x and y, the designed metamaterial exhibits an anisotropic optical response, involving both types of collective modes. For y-polarized normal incidence, a reflective collective mode of the second order ($q = 2$ in Equation (7)) arises at the resonance wavelength. **Figure 6**a,b shows the reflection, transmission, and absorption from a structure of 10 layers, for x-polarized and y-polarized normal incidence, re-

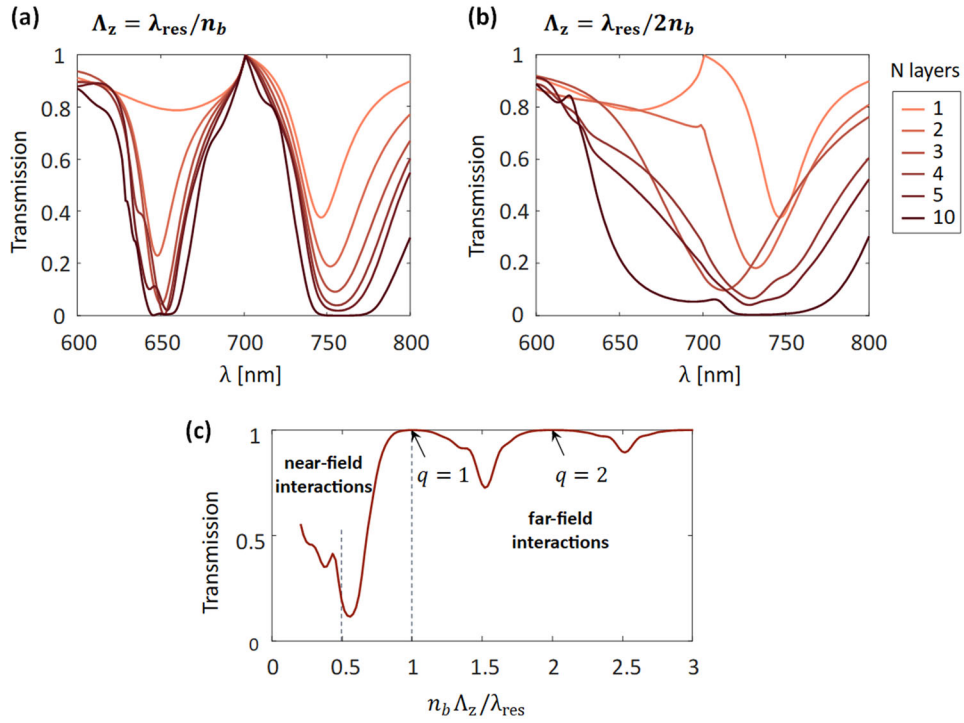

Figure 5. a,b) Transmission from a metamaterial with increasing number of layers *N* and periodicities $\Lambda_x = 300$ nm and $\Lambda_y = 480$ nm, for two different cases, a) $\Lambda_z = \lambda_{res}/n_b = 480$ nm when momentum matching along the *y*-direction is achieved, supporting a transmissive volume collective mode, and b) $\Lambda_z = \lambda_{res}/2\,n_b = 240$ nm when momentum matching along the *y*-direction is not achieved. c) Transmission from a stack of 5 layers at the resonance wavelength as function of $n_b\Lambda_z/\lambda_{res}$, where the arrows indicate the transmissive volume collective modes, according to Equation (10), and the dashed lines indicate the two values of Λ_z in (a) and (b). Taken from CDA calculations.

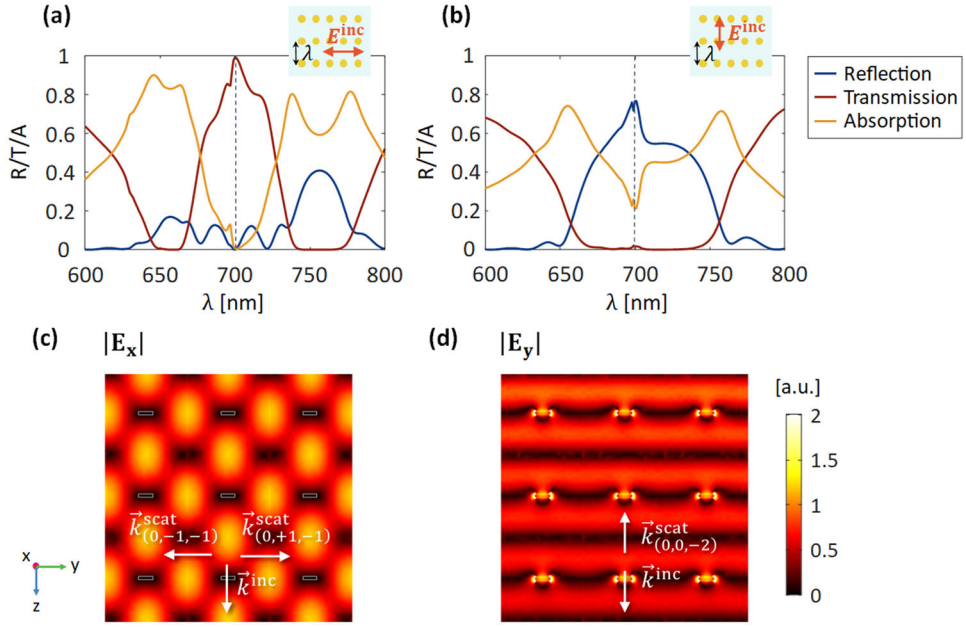

Figure 6. An anisotropic metamaterial that supports different volume collective modes according to the incident wave polarization, consisting of 10 layers with periodicities $\Lambda_x = 300$ nm and $\Lambda_y = \Lambda_z = \lambda_{res}/n_b = 480$ nm. a,b) Reflection, transmission, and absorption for a) *x*-polarized and b) *y*-polarized normal incident wave, taken from finite-element simulations. The insets show a top view of the structure in the x-y plane. c,d) A cross-section view of the amplitude of c) E_x for *x*-polarized incidence and d) E_y for *y*-polarized incidence, at the resonance wavelength $\lambda_{res} = 700$ nm, taken from finite-element simulations.

spectively. It shows that in addition to the aforementioned transparency window at the resonance wavelength for *x*-polarized light, the opposite *y*-polarized light will be strongly reflected from the metamaterial with minimal loss. For *x*-polarized incidence, the destructive interference of the lattice matched scattered waves with the incident wave at the nanoparticles' location can be seen from the standing wave pattern in Figure 6c, which leads to the cancelation of their dipole moment. For *y*-polarized incidence, the collective excitation of the dipole moments can be seen from the amplitude of E_y, as depicted in Figure 6d.

The realization of the designed 3D metamaterials can be achieved by the fabrication and stacking of metasurface layers. Each metasurface layer, consisting of gold nanodisks, is fabricated by a standard E-beam lithography, followed by evaporation of gold and a lift-off. Then, a spacer layer of silica for example is grown on top of the nanodisks, at a thickness of Λ_z. The process is repeated until the desired number of layers is achieved.[19,22,34] As a consequence of the sequential method of fabrication, the physical parameters of the nanodisks array might vary from layer to layer due to inconsistencies between the different lithography processes, as well as misalignments in the displacement of the layers. In Sections 2 and 3, Supporting Information, we give an analysis of the effect of these variations, based on CDA simulations, for the two types of metamaterials depicted in Figures 2 and 5. The reflective volume collective mode, supported by the structure depicted in Figure 2, depends only on the distance between the layers Λ_z, where Λ_x and Λ_y are subwavelength. Therefore, misalignments between the layers do not affect the behavior of this mode, as can be seen in Figure S3, Supporting Information. Variations of the nanodisks between the different layers will shift their resonances from the central wavelength of the volume collective mode, and the overall scattering will decrease. However, assuming a reasonable maximum error of 10 nm in the nanodisks size, the spectral behavior of the mode is maintained, as can be seen in Figure S5, Supporting Information. The transmissive volume collective mode, supported by the structure depicted in Figure 5, will not be affected by variations in the nanodisks size, due to the cancellation of the nanodisks dipole moment, as discussed before. This is evident from Figure S6, Supporting Information. However, since the transmissive mode depends on both Λ_z and Λ_y, it will be affected by misalignments between the layers, as can be seen in Figure S4, Supporting Information. Although the metamaterial is not entirely transparent at the designed wavelength in this case, a window of high transmission still emerges. This is the worst-case scenario of lack of alignment. Improving the alignment between the layers, for example by using designated markers in the fabrication, will further enhance the performance of this mode.

We point out that the studied configurations in this work assumed identical nanoparticles under normal incidence, however volume collective modes can be supported in oblique incidence as well, under the momentum conservation condition in Equation (5). In addition, the reported collective phenomenon can include other types of meta-atoms, such as anisotropic scatterers that induce polarization-dependent response,[19,22] as well as nonlinear nanoparticles, where collective modes in the system have the potential to substantially increase the efficiency of nonlinear frequency conversion processes.[23,35] Moreover, the concept of finding collective modes through a study of the system's eigenmodes can be further extended to stacks of metasurfaces with different optical responses, realizing optical platforms with multiple functionalities.[21,36–38]

4. Conclusions

We have revealed intriguing optical anomalies due to two types of volume collective modes in 3D plasmonic metamaterials. One type strongly reflects the incoming light and substantially decreases the plasmonic absorption, while locking the resonant response of the nanoresonators throughout the volume of the metamaterial at an exceptionally high quality factor. Another type excites lattice matched scattered waves within the volume that can lead to an exceptional transparency window in the spectrum. Our findings show how subwavelength inclusions can be artificially designed in a 3D space to be collectively excited across the volume and achieve unique optical properties. We believe that the study of volume collective modes in artificial nano-engineered materials can unlock further anomalous optical phenomena based on light-matter interactions, and has the potential to realize metamaterial-based optical devices with highly advanced functionalities.

Supporting Information

Supporting Information is available from the Wiley Online Library or from the author.

Acknowledgements

This research was supported by the Israel Science Foundation (grant No. 581/19).

Conflict of Interest

The authors declare no conflict of interest.

Data Availability Statement

The data that support the findings of this study are available from the corresponding author upon reasonable request.

Keywords

3D metamaterials, coherent scattering, collective excitation, plasmonic nanoparticles, volume collective modes

Received: September 4, 2022
Revised: November 9, 2022
Published online:

[1] N. Meinzer, W. L. Barnes, I. R. Hooper, *Nat. Photonics* **2014**, *8*, 889.
[2] M. Kadic, G. W. Milton, M. van Hecke, M. Wegener, *Nat. Rev. Phys.* **2019**, *1*, 198.

[3] A. Christ, S. G. Tikhodeev, N. A. Gippius, J. Kuhl, H. Giessen, *Phys. Rev. Lett.* **2003**, *91*, 183901.
[4] Y. Fan, Z. Wei, H. Li, H. Chen, C. M. Soukoulis, *Phys. Rev. B: Condens. Matter Mater. Phys.* **2013**, *88*, 241403.
[5] N. S. Mueller, Y. Okamura, B. G. M. Vieira, S. Juergensen, H. Lange, E. B. Barros, F. Schulz, S. Reich, *Nature* **2020**, *583*, 780.
[6] B. Auguié, W. L. Barnes, *Phys. Rev. Lett.* **2008**, *101*, 143902.
[7] Y. Chu, E. Schonbrun, T. Yang, K. B. Crozier, *Appl. Phys. Lett.* **2008**, *93*, 181108.
[8] M. B. Ross, C. A. Mirkin, G. C. Schatz, *J. Phys. Chem. C* **2016**, *120*, 816.
[9] M. S. Bin-Alam, O. Reshef, Y. Mamchur, M. Z. Alam, G. Carlow, J. Upham, B. T. Sullivan, J. M. Ménard, M. J. Huttunen, R. W. Boyd, K. Dolgaleva, *Nat. Commun.* **2021**, *12*, 974.
[10] L. Michaeli, S. Keren-Zur, O. Avayu, H. Suchowski, T. Ellenbogen, *Phys. Rev. Lett.* **2017**, *118*, 243904.
[11] Y. Liang, K. Koshelev, F. Zhang, H. Lin, S. Lin, J. Wu, B. Jia, Y. Kivshar, *Nano Lett.* **2020**, *20*, 6351.
[12] A. I. Aristov, M. Manousidaki, A. Danilov, K. Terzaki, C. Fotakis, M. Farsari, A. V. Kabashin, *Sci. Rep.* **2016**, *6*, 25380.
[13] L. Sun, H. Lin, K. L. Kohlstedt, G. C. Schatz, C. A. Mirkin, *Proc. Natl. Acad. Sci. U. S. A.* **2018**, *115*, 7242.
[14] Z. Guo, H. Jiang, H. Chen, *J. Appl. Phys.* **2020**, *127*, 071101.
[15] A. Karnieli, Y. Li, A. Arie, *Front. Phys.* **2022**, *17*, 12301.
[16] A. Krasnok, M. Tymchenko, A. Alù, *Mater. Today* **2018**, *21*, 8.
[17] S. Chen, G. Li, K. W. Cheah, T. Zentgraf, S. Zhang, *Nanophotonics* **2018**, *7*, 1013.
[18] I. Fernandez-Corbaton, C. Rockstuhl, P. Ziemke, P. Gumbsch, A. Albiez, R. Schwaiger, T. Frenzel, M. Kadic, M. Wegener, *Adv. Mater.* **2019**, *31*, 1807742.
[19] Y. Zhao, M. A. Belkin, A. Alù, *Nat. Commun.* **2012**, *3*, 870.
[20] R. Taubert, D. Dregely, T. Stroucken, A. Christ, H. Giessen, *Nat. Commun.* **2012**, *3*, 691.
[21] N. K. Grady, J. E. Heyes, D. R. Chowdhury, Y. Zeng, M. T. Reiten, A. K. Azad, A. J. Taylor, D. A. R. Dalvit, H. T. Chen, *Science* **2013**, *340*, 1304.
[22] J. Sperrhake, M. Decker, M. Falkner, S. Fasold, T. Kaiser, I. Staude, T. Pertsch, *Opt. Express* **2019**, *27*, 1236.
[23] T. Stolt, J. Kim, S. Héron, A. Vesala, Y. Yang, J. Mun, M. Kim, M. J. Huttunen, R. Czaplicki, M. Kauranen, J. Rho, P. Genevet, *Phys. Rev. Lett.* **2021**, *126*, 033901.
[24] J. B. Khurgin, *Nat. Nanotechnol.* **2015**, *10*, 2.
[25] C. Cherqui, M. R. Bourgeois, D. Wang, G. C. Schatz, *Acc. Chem. Res.* **2019**, *52*, 2548.
[26] V. G. Kravets, A. V. Kabashin, W. L. Barnes, A. N. Grigorenko, *Chem. Rev.* **2018**, *118*, 5912.
[27] S. Steshenko, F. Capolino, P. Alitalo, S. Tretyakov, *Phys. Rev. E: Stat., Nonlinear, Soft Matter Phys.* **2011**, *84*, 016607.
[28] P. Lunnemann, I. Sersic, A. F. Koenderink, *Phys. Rev. B: Condens. Matter Mater. Phys.* **2013**, *88*, 245109.
[29] M. Decker, I. Staude, M. Falkner, J. Dominguez, D. N. Neshev, I. Brener, T. Pertsch, Y. S. Kivshar, *Adv. Opt. Mater.* **2015**, *3*, 813.
[30] Y. Zhao, N. Engheta, A. Alù, *Metamaterials* **2011**, *5*, 90.
[31] L. Rayleigh, *Proc. R. Soc. London, Ser. A* **1907**, *79*, 399.
[32] A. Hessel, A. A. Oliner, *Appl. Opt.* **1965**, *4*, 1275.
[33] L. Michaeli, H. Suchowski, T. Ellenbogen, *Laser Photonics Rev.* **2020**, *14*, 1900204.
[34] R. Czaplicki, A. Kiviniemi, M. J. Huttunen, X. Zang, T. Stolt, I. Vartiainen, J. Butet, M. Kuittinen, O. J. F. Martin, M. Kauranen, *Nano Lett.* **2018**, *18*, 7709.
[35] N. Segal, S. Keren-Zur, N. Hendler, T. Ellenbogen, *Nat. Photonics* **2015**, *9*, 180.
[36] C. Menzel, J. Sperrhake, T. Pertsch, *Phys. Rev. A* **2016**, *93*, 063832.
[37] S. Chen, Y. Zhang, Z. Li, H. Cheng, J. Tian, *Adv. Opt. Mater.* **2019**, *7*, 1801477.
[38] G. Hu, M. Wang, Y. Mazor, C. W. Qiu, A. Alù, *Trends Chem.* **2021**, *3*, 342.